

## Biochemical Characterization of the C<sub>4</sub>-Dicarboxylate Transporter DctA from *Bacillus subtilis*<sup>∇</sup>

Maarten Groeneveld, Ruud G. J. Detert Oude Weme, Ria H. Duurkens, and Dirk Jan Slotboom\*

Department of Biochemistry, University of Groningen, Groningen Biomolecular Science and Biotechnology Institute, Nijenborgh 4, 9747 AG Groningen, Netherlands

Received 8 February 2010/Accepted 22 March 2010

**Bacterial secondary transporters of the DctA family mediate ion-coupled uptake of C<sub>4</sub>-dicarboxylates. Here, we have expressed the DctA homologue from *Bacillus subtilis* in the Gram-positive bacterium *Lactococcus lactis*. Transport of dicarboxylates *in vitro* in isolated membrane vesicles was assayed. We determined the substrate specificity, the type of cotransported ions, the electrogenic nature of transport, and the pH and temperature dependence patterns. DctA was found to catalyze proton-coupled symport of the four C<sub>4</sub>-dicarboxylates from the Krebs cycle (succinate, fumarate, malate, and oxaloacetate) but not of other mono- and dicarboxylates. Because (i) succinate-proton symport was electrogenic (stimulated by an internal negative membrane potential) and (ii) the divalent anionic form of succinate was recognized by DctA, at least three protons must be cotransported with succinate. The results were interpreted in the light of the crystal structure of the homologue aspartate transporter Glt<sub>ph</sub> from *Pyrococcus horikoshii*.**

The DctA family is one of several diverse families of secondary transporters that catalyze the uptake of C<sub>4</sub>-dicarboxylates from the Krebs cycle in bacteria (16, 27). In *Escherichia coli*, DctA mediates the uptake of succinate, fumarate, and malate under aerobic conditions; genomic disruption of *dctA* in *E. coli* prevents growth with malate or fumarate as the sole carbon source, and the mutant grows poorly on succinate (5). Similarly, a *dctA* knockout mutant of *Bacillus subtilis* cannot grow with succinate or fumarate as the sole carbon source (1). DctA plays a major role in the symbiotic relationship between nitrogen-fixing rhizobia (43) and root nodule-forming plants (30, 37, 38). Transport assays with *Sinorhizobium meliloti* cells showed previously that in addition to succinate, malate, and fumarate, orotate is transported and that a range of other substrates such as succinamic acid and succinamide may be transported, because they inhibit the transport of orotate (42). In *Corynebacterium glutamicum*, malate transport by DctA is inhibited by  $\alpha$ -ketoglutarate, oxaloacetate, and glyoxylate, indicating that these compounds may be substrates also (41).

DctA transporters belong to a large family of secondary transporters (the DAACS [dicarboxylate/amino acid:cation symporter] family), which also comprises well-characterized glutamate/aspartate transporters and neutral amino acid transporters (32, 33). While DctA-type dicarboxylate transporters are found only in bacteria, glutamate/aspartate transporters of the DAACS family are found both in prokaryotes (e.g., GltT in *Bacillus stearothermophilus*, GltP in *E. coli*, and Glt<sub>ph</sub> in *Pyrococcus horikoshii* [2, 7, 34]) and in higher eukarya, where they play a pivotal role in the reuptake of the excitatory neurotransmitter glutamate from the synaptic cleft (4). Neutral amino

acid (alanine, serine, and threonine) transporters are found in mammals (see, e.g., references 36 and 44) as well as bacteria (17).

Secondary transporters of the DAACS family use (electro) chemical gradients of cations across the membrane to drive transport. The type of cotransported ions varies among family members: eukaryotic glutamate transporters couple the transport of glutamate to the symport of one proton and three sodium ions and the antiport of one potassium ion (24, 45). Bacterial and archaeal glutamate transporters utilize either sodium ions or protons for symport (2) and are independent of potassium ions (28, 31). The bacterial and mammalian neutral amino acid transporters are sodium ion coupled. Glutamate/aspartate transporters and bacterial serine/threonine transporters (SstTs) are electrogenic, but mammalian neutral amino acid transporters are obligate electroneutral amino acid antiporters (44).

Insight into the structure-function relationships of the DAACS family members has greatly increased since crystal structures of the *P. horikoshii* aspartate transporter Glt<sub>ph</sub> have been determined (2, 29, 40). The protein consists of eight membrane-spanning helices and two reentrant regions (helical hairpins HP1 and HP2) (40). The C-terminal part of the protein (helices 7 and 8 and HP1 and HP2) is most strongly conserved with respect to other family members and binds the substrate and cotransported ions, with HP1 and HP2 functioning as lids that allow alternating access to the substrate- and ion-binding sites from either side of the membrane (3, 29). Glt<sub>ph</sub> forms a homotrimeric complex in which each protomer functions independently of the other subunits (11, 12, 18, 19, 23). The fold and oligomeric state are likely to be conserved throughout the family.

Whereas the transport mechanisms of bacterial glutamate and neutral amino acid transporters of the DAACS family have been studied extensively *in vitro*, the C<sub>4</sub>-dicarboxylate transporters of the DAACS family (DctA proteins) have been studied using whole cells only. To fully characterize these

\* Corresponding author. Mailing address: Department of Biochemistry, University of Groningen, Groningen Biomolecular Science and Biotechnology Institute, Nijenborgh 4, 9747 AG Groningen, Netherlands. Phone: 31 (0)50 363 4187. Fax: 31 (0)50 363 4165. E-mail: D.J.Slotboom@rug.nl.

<sup>∇</sup> Published ahead of print on 2 April 2010.

transporters, *in vitro* activity assays using either membrane vesicles or proteoliposomes containing purified protein are necessary. In such assays, the internal and external buffer compositions can be controlled, thus allowing manipulation of the chemical ion gradients and the electrical potential across the membrane. Here, we present the first biochemical characterization of a DctA family member in membrane vesicles. We have studied the DctA homologue from *B. subtilis*, which is annotated as DctP (1) but which we propose to rename DctA to reflect the homology to other DctA proteins. *B. subtilis* DctA (DctA<sub>Bs</sub>) has 30 to 32% sequence identity to the aspartate transporter Glt<sub>Pn</sub> and human excitatory amino acid transporter (EAAT) family members, over 40% sequence identity to the characterized bacterial glutamate transporters from *E. coli* and *B. stearothermophilus*, and 41 and 56% identity to DctA homologues from *C. glutamicum* and *E. coli*, respectively. We determined the substrate specificity of DctA<sub>Bs</sub>, the type of cotransported ions, the electrogenic nature of transport, and the pH and temperature dependence patterns.

## MATERIALS AND METHODS

**Chemicals.** Restriction enzymes and polymerases were purchased from Fermentas Life Sciences (Burlington, CA). [<sup>14</sup>C]succinate (1.85 MBq/ml [2.04 GBq/mmol]) was purchased from ARC Radiochemicals (St. Louis, MO). Lipids were purchased from Avanti Polar Lipids (Alabaster, AL). All chemicals were of analytical grade.

**DNA manipulations.** The *dctA* gene from *B. subtilis* was amplified from genomic DNA by PCR using Phusion polymerase according to the manufacturer's instructions. For expression in *Lactococcus lactis*, the PCR products were cloned into vector pRE-Nlic, essentially as described by Geertsma and Poolman (9). The pRE-Nlic vector was converted into a plasmid for expression in *L. lactis* by the vector-backbone exchange (VBeX) method (9). Vectors were designed in such a way that an N-terminal decahistidine tag followed by a tobacco etch virus (TEV) protease cleavage site was added to the protein product. DNA sequencing by Service XS (Leiden, Netherlands) confirmed that no unwanted mutations had occurred.

**Expression and purification of DctA<sub>Bs</sub>.** DctA<sub>Bs</sub> was expressed in *L. lactis* NZ9000 cells (21) grown on M17 medium (Oxoid, Basingstoke, United Kingdom) supplemented with 1% glucose at a constant pH (6.5) and temperature (30°C). Expression was induced by the addition of nisin A to a 1:5,000 (vol/vol) dilution of the supernatant from a stationary-phase *L. lactis* NZ9700 culture at an optical density at 660 nm of ~1.5 (20). Two hours after induction, cells were harvested with a Beckman JLA 8.1000 rotor at a relative centrifugal force [RCF] of 10,000 for 10 min at 4°C and resuspended in 20 mM Tris-HCl (pH 8). DNase (10 μg/ml), phenylmethylsulfonyl fluoride (PMSF; 200 μM), and MgSO<sub>4</sub> (1 mM) were added, and cells were passed twice through a cell disrupter at 45,000 lb/in<sup>2</sup> (Constant Systems Ltd., Daventry, United Kingdom) and cooled at 4°C. Unbroken cells and cell debris were pelleted using a Harrier 18/80 swing-out centrifuge at an RCF of 5,000 for 25 min at 4°C, and the supernatant was subjected to ultracentrifugation using a Beckman 50.2 Ti rotor at an RCF of 150,000 for 90 min at 4°C. Membrane pellets were resuspended in 20 mM Tris-HCl (pH 8) and stored at -80°C. The protein concentrations in the membranes were determined using Bradford reagent with bovine serum albumin as a standard.

For protein purification (7), membrane vesicles were solubilized in buffer A (50 mM Tris-HCl [pH 8.0], 300 mM NaCl), containing 15 mM imidazole (pH 8.0) and 1% *n*-dodecyl-β-D-maltopyranoside (DDM), at a final protein concentration of 5 mg/ml. After incubation on ice for 45 min with occasional gentle shaking, the solution was centrifuged with a Beckman TLA 100.4 rotor at an RCF of 267,000 for 15 min at 4°C. Supernatants were incubated on a rotating platform for 60 min at 4°C with a nickel-Sepharose slurry (Fast Flow; GE Healthcare) preequilibrated with buffer A containing 15 mM imidazole, pH 8.0. The mixture was loaded onto a Bio-Rad Poly-Prep column, and unbound protein was allowed to flow through. The column was washed with 20 column volumes of buffer A supplemented with 60 mM imidazole and 0.04% DDM. Protein was eluted from the column in three fractions of 300, 500, and 500 μl by using buffer A supplemented with 500 mM imidazole, pH 8.0, and 0.04% DDM. The second elution fraction from the affinity chromatography contained most of the purified protein

and was loaded onto a Superdex-200 gel filtration column using 20 mM potassium phosphate, pH 7.0, 150 mM NaCl, and 0.04% DDM as eluents.

Throughout the purification procedure, samples were taken and analyzed by sodium dodecyl sulfate (SDS)-12.5% polyacrylamide gel electrophoresis. Gels were stained using Serva Blue G Coomassie brilliant blue.

**Fused membrane vesicles.** *L. lactis* membrane vesicles were mixed in a 1:10 (wt/wt) ratio of protein (from the membrane vesicle preparation) to lipid (from liposomes) with liposomes made from *E. coli* polar lipids and egg phosphatidylcholine (3:1, wt/wt) that had been extruded nine times through a 400-nm-pore-size polycarbonate filter by using a miniextruder (Hamilton, Bonaduz, Switzerland). The mixture was frozen in liquid nitrogen, thawed three times, and subjected to centrifugation with a Beckman TLA 100.4 rotor at an RCF of 267,000 for 20 min at 4°C. Fused membranes were then resuspended in the luminal buffer of choice (see the figure legends), again frozen and thawed three times, and stored in liquid nitrogen. Freezing, thawing, and subsequent extrusion (see below) were used to load the vesicles with the desired buffer.

**Transport assays using fused membrane vesicles.** Fused membranes were thawed, extruded as described above, and centrifuged with a Beckman TLA 100.4 rotor at an RCF of 267,000 for 20 min at 4°C. Membranes were resuspended in the internal (luminal) buffer to a total protein concentration of 12.5 μg/μl. In transport assays, fused membrane vesicles were diluted 100× into 200 μl of external buffer (described in Results) supplemented with [<sup>14</sup>C]succinate (a 3.1 μM concentration, unless otherwise indicated) and, if applicable, 0.5 μM valinomycin (3 mM stock solution in ethanol). All assays were performed at 25°C, except when otherwise indicated, and internal and external buffers were isosmotic. Transport reactions were stopped by the addition of 2 ml of ice-cold 100 mM LiCl, followed by rapid filtration with BA-85 nitrocellulose filters and an additional wash step with lithium chloride. Levels of radioactivity were determined by the addition of 2 ml of Emulsifier-Scintillator Plus liquid (PerkinElmer, Waltham, MA) and analysis with a PerkinElmer Tri-Carb 2800 TR isotope counter.

## RESULTS

**Expression and purification of DctA<sub>Bs</sub>.** Initially we aimed at the purification of DctA<sub>Bs</sub> and reconstitution in proteoliposomes. A histidine-tagged variant of the protein was expressed in the Gram-positive host *L. lactis* (22). The DctA<sub>Bs</sub> protein was extracted from *L. lactis* membrane vesicles by solubilization using the detergent DDM and purified by nickel affinity and size exclusion chromatography (Fig. 1A). The protein eluted at a volume of ~11 ml from the size exclusion column (Fig. 1B). The trimeric prokaryotic glutamate/aspartate transporters of the DAACS family elute at similar volumes (10, 39, 40), indicating that DctA<sub>Bs</sub> is probably also a homotrimer. However, the size exclusion chromatogram showed that the protein was prone to aggregation in detergent solution. Static light-scattering (size exclusion chromatography-multiangle laser light-scattering [SEC-MALLS]) analysis of DctA<sub>Bs</sub> indeed showed that the elution peak was not monodisperse, but the results were consistent with a trimeric oligomeric state of the protein in the main peak (data not shown). Varying the buffer composition (by the addition of glycerol or salt) or the pH (from 6 to 8.5) did not improve the stability of the protein, nor did the addition of a substrate (succinate) to the buffers throughout the purification. The chromatogram for DctA<sub>Bs</sub> shown in Fig. 1B was the best obtained.

The DctA<sub>Bs</sub> protein from the peak fraction around the elution volume of 11 ml was used in reconstitution trials. In addition, DctA<sub>Bs</sub> that had been partially purified by only metal affinity chromatography was also used in reconstitution trials. All attempts to functionally reconstitute the purified protein into proteoliposomes failed. Different detergents (maltoside series and octyl glucoside) and reconstitution protocols (deter-

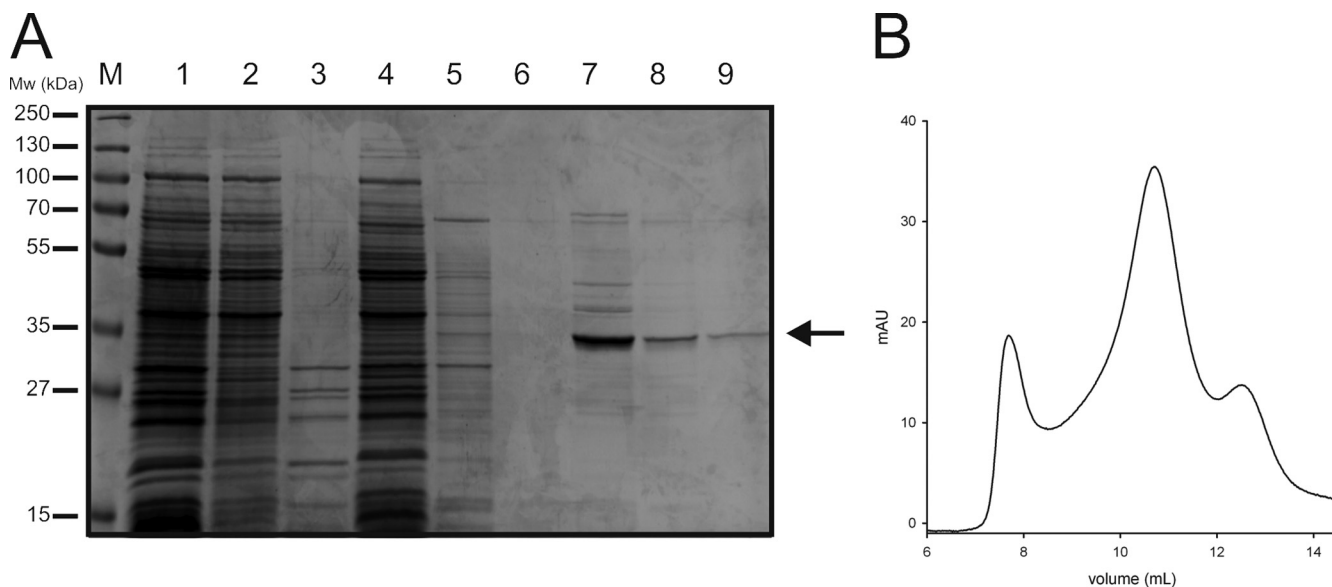


FIG. 1. Purification of DctA<sub>Bs</sub>. (A) Protein samples from different steps throughout the purification were run on an SDS–12.5% polyacrylamide gel, which was stained with Coomassie brilliant blue. Lanes: 1, membrane vesicles (10  $\mu$ g of protein); 2, DDM-soluble fraction; 3, insoluble fraction; 4, flowthrough from the nickel-Sepharose column; 5, wash fraction from the Ni-Sepharose column; 6 to 8, three elution fractions from the nickel-Sepharose column; and 9, peak fraction (at an elution volume of  $\sim$ 11 ml) from the size exclusion chromatography step. The arrow indicates DctA<sub>Bs</sub>. M, markers; Mw, molecular mass. (B) The peak elution fraction from the nickel-Sepharose column (lane 7) was subjected to size exclusion chromatography with a Superdex-200 column. The chromatogram is shown.

gent removal by rapid dilution [14] and BioBead adsorption [8]) were tested, but none resulted in functional protein.

**DctA<sub>Bs</sub> is a proton-coupled succinate transporter.** It was possible that the failure to reconstitute DctA<sub>Bs</sub> in an active form had been caused by instability of the protein in detergent solution. To avoid the need for solubilization of DctA<sub>Bs</sub> by detergents, *in vitro* transport assays using membrane vesicles

prepared from *L. lactis* cells overexpressing DctA<sub>Bs</sub> were attempted. We monitored the uptake of radiolabeled succinate into membrane vesicles in the presence of chemical gradients for sodium ions and protons and a negative membrane potential ( $\Delta\mu_{H^+}$ ,  $\Delta\mu_{Na^+}$ , and  $\Delta\Psi$ , respectively) (Fig. 2). Rapid succinate transport in membrane vesicles containing DctA<sub>Bs</sub> was observed. Transport was DctA mediated, because no accumu-

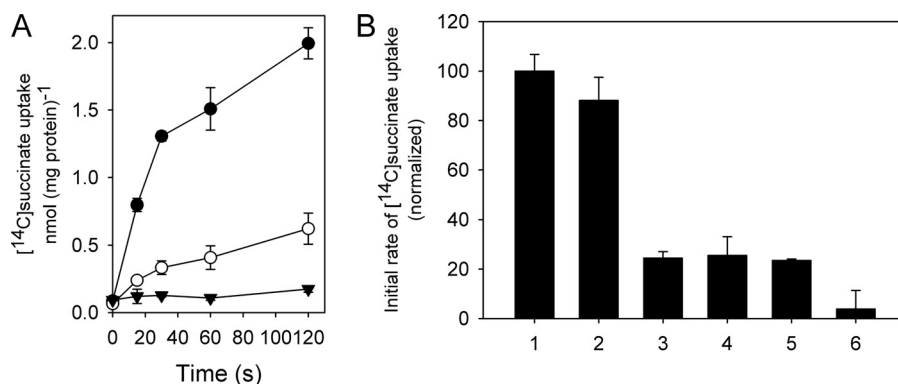


FIG. 2. Succinate transport by DctA<sub>Bs</sub> in membrane vesicles. (A) Membrane vesicles containing DctA<sub>Bs</sub> (circles) or ThiT (negative control; triangles) were loaded with 100 mM K-HEPES (pH 7.5). The vesicles were diluted 100-fold in an isosmotic Na-MES buffer, pH 5.5 (consisting of  $\sim$ 135 mM MES [morpholineethanesulfonic acid] adjusted to pH 5.5 with NaOH), containing 3.1  $\mu$ M [<sup>14</sup>C]succinate in the presence (closed symbols) or absence (open symbols) of 0.5  $\mu$ M valinomycin. In this way, chemical gradients for protons and sodium ions ( $\Delta\mu_{H^+}$  and  $\Delta\mu_{Na^+}$ ) were created. In the presence of valinomycin, an additional K<sup>+</sup> diffusion potential,  $\Delta\Psi$  (Nernst potential,  $-118$  mV), was created. (B) Initial [<sup>14</sup>C]succinate transport rates in the presence of various gradients. Columns correspond to the presence of gradients as follows: 1,  $\Delta\mu_{H^+}$ ,  $\Delta\mu_{Na^+}$ , and  $\Delta\Psi$ ; 2,  $\Delta\mu_{H^+}$  and  $\Delta\Psi$ ; 3,  $\Delta\mu_{H^+}$  and  $\Delta\mu_{Na^+}$ ; 4,  $\Delta\mu_{H^+}$ ; 5,  $\Delta\mu_{Na^+}$  and  $\Delta\Psi$ ; and 6, negative control. Initial transport rates were calculated from data for the 15-s time point (see panel A). Data were normalized, and the highest measured rate [ $47.4$  pmol (mg protein  $\cdot$  s)<sup>-1</sup>] was set at 100%. Proton and sodium ion gradients ( $\Delta\mu_{H^+}$  and  $\Delta\mu_{Na^+}$ ) in the presence or absence of  $\Delta\Psi$  were created as described in the legend to panel A. To create  $\Delta\mu_{H^+}$  in the absence of  $\Delta\mu_{Na^+}$ , external methylglucamine-MES buffer (pH 5.5) was used instead of Na-MES buffer. Again, the addition of valinomycin was used to create a K<sup>+</sup> diffusion membrane potential ( $\Delta\Psi$ ) where indicated. To create  $\Delta\mu_{Na^+}$  and  $\Delta\Psi$  in the absence of  $\Delta\mu_{H^+}$ , Na-HEPES (pH 7.5) was used as the external buffer and valinomycin was present. ThiT-harboring vesicles were used as a control in the presence of all three gradients. All data are averages of three independent measurements; error bars indicate standard deviations.

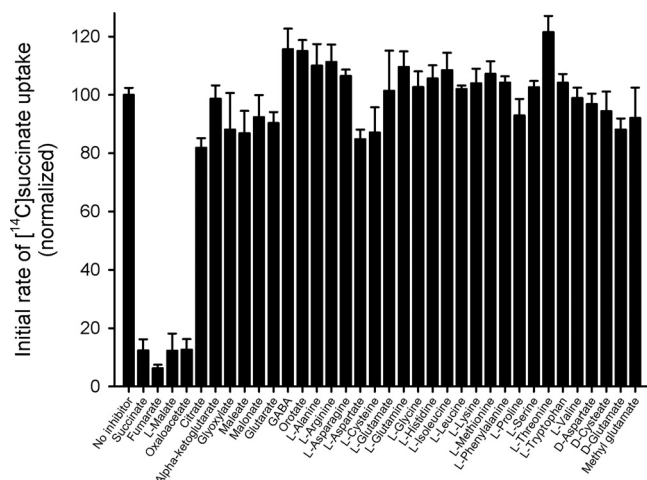


FIG. 3. Succinate transport by DctA<sub>Bs</sub> in membrane vesicles in the presence of putative transport inhibitors. Transport of [<sup>14</sup>C]succinate (3.1 μM) in the presence of Δμ<sub>H<sup>+</sup></sub>, Δμ<sub>Na<sup>+</sup></sub>, and ΔΨ (−118 mV) was measured as described in the legend to Fig. 2A. The external buffer was supplemented with a 50-fold excess of the indicated compounds. Initial transport rates were determined as described in the legend to Fig. 2B and normalized with respect to the rate without inhibitors [100%, corresponding to 37.5 pmol (mg protein · s)<sup>−1</sup>]. Measurements were performed in quadruplicate, and standard deviations are shown.

lation of succinate was observed in membrane vesicles in which the unrelated thiamine transporter ThiT from *L. lactis* was overexpressed (6). To establish which ion gradients were required for transport, we varied the composition of the external buffers. Omission of the sodium ion gradient (Δμ<sub>Na<sup>+</sup></sub>) did not affect transport rates, but when the pHs on the two sides of the membrane were equal, transport rates and accumulation levels were strongly reduced, regardless of the presence of a gradient of sodium ions. An internal negative membrane potential stimulated succinate transport rates and accumulation levels both with and without a pH gradient, indicating that transport by DctA<sub>Bs</sub> was electrogenic, with a net positive charge moving in the same direction as the dicarboxylate substrate.

**Succinate transport by DctA<sub>Bs</sub> is inhibited by other C<sub>4</sub>-dicarboxylates.** To determine the substrate specificity of DctA<sub>Bs</sub>, we tested whether the addition of a 50-fold excess of unlabeled putative substrates inhibited transport of radiolabeled succinate (Fig. 3). Only the addition of the C<sub>4</sub>-dicarboxylates succinate, fumarate, malate, and oxaloacetate strongly inhibited uptake of [<sup>14</sup>C]succinate into the membrane vesicles. The addition of maleate and various C<sub>3</sub>- and C<sub>5</sub>-dicarboxylates did not inhibit transport. None of the natural amino acids were able to inhibit succinate transport. Also, the addition of cysteate, gamma-aminobutyric acid (GABA), orotate, glyoxylate, and α-ketoglutarate had no effect on succinate uptake. It must be noted that the results do not exclude the possibility that the noninhibitory compounds may be low-affinity substrates, because only 170 μM concentrations were used in the inhibition assay. However, as discussed below, a counterflow assay showed that it is very unlikely that the compounds are (low-affinity) substrates of DctA<sub>Bs</sub>.

**Fumarate, oxaloacetate, and malate are substrates for DctA<sub>Bs</sub>.** The results of the inhibition assay (Fig. 3) demonstrated that DctA<sub>Bs</sub> might transport fumarate, malate, and

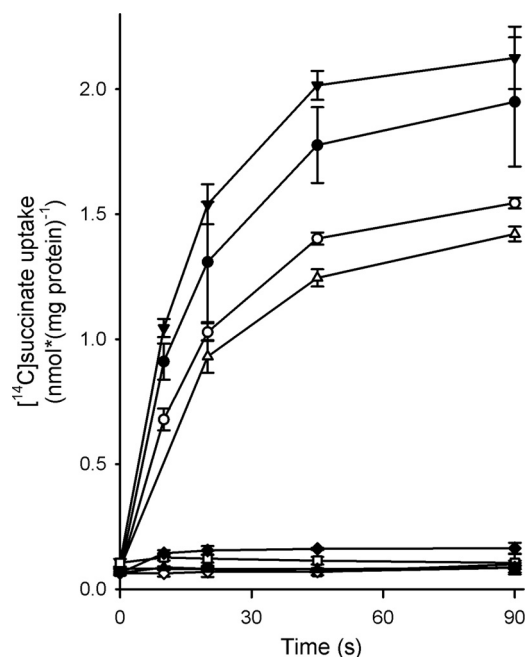


FIG. 4. Succinate counterflow by DctA<sub>Bs</sub>. Membrane vesicles were loaded with 50 mM potassium phosphate (pH 7.0) supplemented with 1 mM succinate (closed circles), fumarate (open circles), malate (closed triangles), oxaloacetate (open triangles), maleate (open squares), citrate (closed squares), or orotate (closed diamonds) and diluted 200-fold in external buffer (50 mM potassium phosphate, pH 7.0) supplemented with 3.1 μM [<sup>14</sup>C]succinate. As a negative control, membrane vesicles that were not loaded with any substrate (open diamonds) or vesicles loaded with 1 mM succinate (crosses) in which ThiT was expressed were used. Measurements were done in triplicate; error bars indicate standard deviations.

oxaloacetate. On the other hand, these compounds could also be competitive inhibitors that bind to the transporter without being transported themselves and, thus, block transport of radiolabeled succinate. To establish whether fumarate, oxaloacetate, and malate were indeed transported by DctA<sub>Bs</sub>, we used a counterflow assay. Membrane vesicles were loaded with 1 mM unlabeled (putative) substrate and diluted in the same buffer containing radiolabeled succinate. If the unlabeled dicarboxylate was indeed transported, exchange of the internal (unlabeled) substrate and external (labeled) succinate would lead to accumulation of [<sup>14</sup>C]succinate, due to the concentration gradient across the membrane. In the counterflow experiments, internalization of the radiolabeled substrate was observed when membrane vesicles were loaded with succinate (demonstrating homologous counterflow) (Fig. 4). Also, the presence of malate, fumarate, or oxaloacetate in the lumina of the membrane vesicles resulted in uptake of radiolabeled succinate into the vesicles. The presence of orotate, citrate, and maleate in the lumina of the vesicles did not result in the induction of succinate counterflow by DctA<sub>Bs</sub>, nor did the presence of aspartate, glyoxylate, or α-ketoglutarate (data not shown). We also did not observe succinate counterflow when no substrate was added to the internal buffer. Control membranes in which ThiT was expressed instead of DctA<sub>Bs</sub> also did not show counterflow of the radiolabeled substrate, regardless of the presence of the internal substrate. DctA<sub>Bs</sub> thus appears

to be specific for a narrow set of  $C_4$ -dicarboxylates. The counterflow assay also showed that aspartate, glyoxylate,  $\alpha$ -ketoglutarate, orotate, citrate, and maleate are not low-affinity substrates of DctA<sub>Bs</sub> because they were not transported even though they were present at high (1 mM) concentrations.

**pH dependence of DctA.** The experimental findings presented in Fig. 2 indicate that DctA<sub>Bs</sub> couples succinate transport to protons and not to sodium ions. This observation corresponds with results obtained for DctA of *C. glutamicum* in a whole-cell experimental setup (41). To gain more insight into both the optimal pH for transport by DctA and the protonation state of the transported dicarboxylate, we measured the pH dependence of succinate transport into membrane vesicles. Interpretation of the pH dependence of succinate transport by DctA<sub>Bs</sub> is complicated because (i) protons are substrates (co-transported ions), (ii) the protonation state of the dicarboxylate substrates depends on the pH, and (iii) there may be other (regulatory) sites on the protein which can be protonated and the protonation state of which may affect activity. We performed three experiments to study the pH dependence of DctA<sub>Bs</sub> by using both net uptake and counterflow assays.

In the first experiment, we varied the external pH (5.5 or 7) while keeping the internal pH (8) constant. We determined the apparent  $K_m$  and the  $V_{max}$  for succinate transport and found that the transporter follows Michaelis-Menten kinetics, which has also been shown previously for other members of the glutamate transporter family (31, 35). The  $V_{max}$  for succinate transport was approximately 3-fold lower at an external pH of 7 [ $1.4 \text{ nmol (mg protein)}^{-1} \text{ s}^{-1}$ ] than at pH 5.5 [ $3.9 \text{ nmol (mg protein)}^{-1} \text{ s}^{-1}$ ]. This result is consistent with the protons being cosubstrates. Although protonation of a pH-sensitive regulatory site at the extracellular face of the protein could also explain the results, we will show below that such regulation is less likely. The apparent  $K_m$  values for succinate transport were identical within the range of error (means  $\pm$  standard deviations,  $2.8 \pm 1.0 \mu\text{M}$  at pH 5.5 and  $2.6 \pm 1.4 \mu\text{M}$  at pH 7;  $n = 3$ ). The  $pK_a$  values for the two carboxylate groups in succinate are 4.2 and 5.6, respectively. At pH 5.5,  $\sim 60\%$  of succinate is in a protonated state (single or double), whereas at pH 7 this percentage is only  $\sim 4\%$ . The 15-fold decrease in the concentration of the protonated substrate was not reflected in the apparent  $K_m$  values, indicating that the doubly deprotonated form of succinate must be recognized by the transporter. Similar interpretations of apparent  $K_m$  values at different pHs have been made to determine the protonation state of the substrate of a glutamate transporter in *L. lactis* (26). The concentration of divalent anionic succinate is  $\sim 2$ -fold higher at pH 7 than at pH 5.5. The increase was also not reflected in the apparent  $K_m$  values. Although this result could indicate that both protonated and unprotonated forms of succinate were recognized by DctA<sub>Bs</sub>, the experimental error in the determination of the  $K_m$  values was too large to accurately measure a 2-fold difference.

In the second experiment, we varied the external pH from 5 to 7 and simultaneously varied the internal pH from 6 to 8, so that a pH gradient of 1 unit was maintained. Succinate transport rates increased by  $\sim 3$ -fold when the internal pH was raised from 6 to 8 (Fig. 5). The transport rates increased despite a reduction in the concentration of the cosubstrate (protons) on the outside, which as described above, was shown

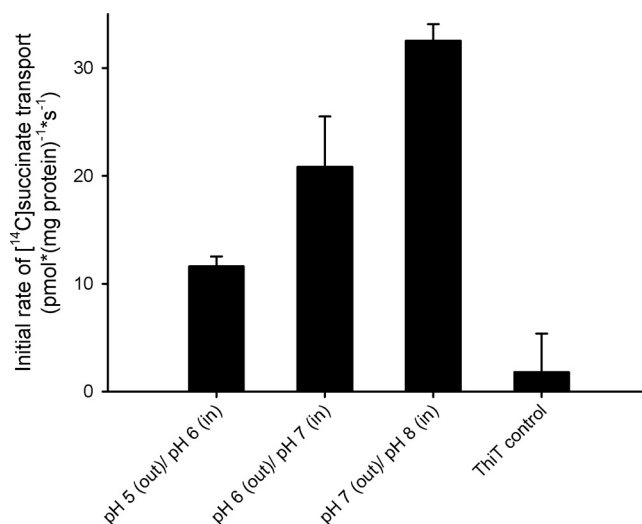


FIG. 5. pH dependence of succinate transport. Membrane vesicles were loaded with a mixture of 50 mM K-MES and 50 mM K-HEPES adjusted to a pH of 6, 7, or 8, and the loaded vesicles were diluted in isosmotic Na-MES–Na-HEPES buffer adjusted to a pH of 5, 6, or 7. The external buffer contained  $3.1 \mu\text{M}$  [ $^{14}\text{C}$ ]succinate and  $0.5 \mu\text{M}$  valinomycin.

in the previous experiment to decrease the transport rate when the internal pH was constant. It is therefore likely that the release of protons on the inside was rate limiting, with the stimulating effect of a higher internal pH being dominant over the inhibitory effect of a higher external pH. An alternative explanation would be that there is a pH-sensitive regulatory site at the intracellular face of the protein resulting in higher activity at alkaline pHs. However, this interpretation would imply that the pH regulation of the protein on the inside and that on the outside work in opposite directions, which is unlikely. The more likely explanation for the observations is that the measured pH dependence directly indicates proton binding on the outside and release on the inside.

In the third experiment, the pH dependence of succinate transport by DctA<sub>Bs</sub> during counterflow with identical pHs on the two sides of the membrane was measured. Maximal succinate counterflow activity was observed at pHs of 6.5 to 7.0 (Fig. 6). At lower pHs and at a pH of 7.5, the rate of exchange was significantly lower. These results suggest that in addition to the substrate, protons are exchanged during the counterflow assay. The observed pH optimum for counterflow activity may thus be a reflection of the stimulation of transport rates by a compromise between (i) high proton concentrations on the outside and (ii) low concentrations on the inside during the counterflow reaction. These results corroborate the interpretation of the findings from the succinate uptake experiments described above, from which we concluded that the measured pH dependence of succinate transport directly represents proton binding on the outside and release on the inside. Exchange of a coupling ion during counterflow has also been observed previously, e.g., with the neutral amino acid transporter ASCT-1 (44) of the DAACS family. In this case, a sodium ion was exchanged.

**A negative membrane potential stimulates succinate transport by DctA.** Succinate transport by DctA<sub>Bs</sub> is electrogenic, as

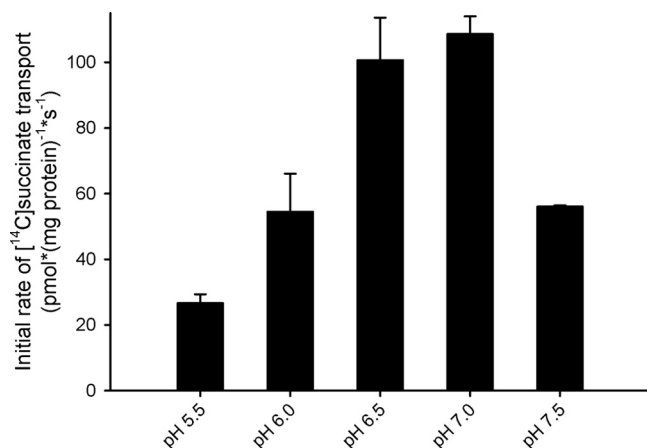


FIG. 6. pH dependence of succinate transport during counterflow. Membrane vesicles were loaded with 50 mM potassium phosphate, supplemented with 1 mM unlabeled succinate, at the indicated pHs. Membrane vesicles were diluted 100-fold in the same external buffer but supplemented with 3.1  $\mu\text{M}$   $[^{14}\text{C}]$ succinate instead of the unlabeled succinate. Error bars indicate the standard deviations, taken from three measurements.

depicted in Fig. 2. To further analyze the effect of the membrane potential on succinate transport by DctA<sub>BS</sub>, the magnitude and sign of the membrane potential were varied. Membrane vesicles were loaded with a buffer containing 10 mM potassium ions. By varying the external concentration of potassium ions, potassium diffusion potentials of different magnitudes were established in the presence of the potassium-selective ionophore valinomycin. In the absence of the ionophore valinomycin, transport was driven solely by the proton gradient and transport rates and accumulation levels were the same regardless of the external potassium ion concentration (data not shown), indicating that the potassium ion concentration does not affect transport. Lack of potassium ion dependence has also been observed previously for other prokaryotic transporters of the DAACS family. In contrast, eukaryotic glutamate transporters require potassium ions as countertransported ions (24, 28, 31, 45).

The addition of valinomycin resulted in an increase of the initial transport rates when the external concentration of potassium was lower than the internal concentration and negative  $\text{K}^+$  diffusion potentials were generated (Fig. 7). When  $\text{K}^+$  concentrations on the two sides of the membrane were equal, the addition of valinomycin also resulted in an increase in transport rates. This result indicates that the net positive charge was translocated inward across the membrane. In the absence of valinomycin, the translocated charge led to the buildup of a positive membrane potential, thus impeding further transport. By clamping the membrane potential at voltages lower than the (positive) equilibrium potential for succinate-proton symport, such impediment was alleviated.

**Temperature optimum and  $Q_{10}$  value.** We measured initial rates of  $[^{14}\text{C}]$ succinate transport by DctA<sub>BS</sub> at temperatures between 10 and 45°C (data not shown). The rates increased when the temperature was raised from 10 up to 40°C. The  $Q_{10}$  value was approximately 1.6 for temperatures between 20 and 40°C, suggesting that significant conformational changes take place during transport. This finding is consistent with results

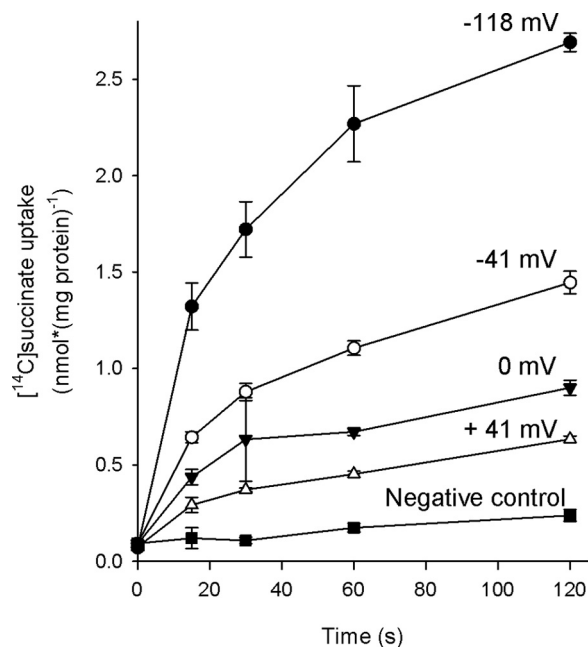


FIG. 7. Succinate transport in the presence of membrane potentials of different magnitudes. Membrane vesicles were loaded with 100 mM Na-HEPES buffer (pH 7.5) supplemented with 10 mM KCl. Membrane vesicles were diluted in external buffer consisting of Na-MES, pH 5.5, and 3.1  $\mu\text{M}$   $[^{14}\text{C}]$ succinate supplemented with 0 mM KCl (closed circles), 2 mM KCl (open circles), 10 mM KCl (closed triangles), or 50 mM KCl (open triangles) in the presence of 0.5  $\mu\text{M}$  valinomycin. The concentration of Na-MES was adjusted to ensure that the external and internal solutions were isosmotic. As a control, succinate transport in membrane vesicles in which ThiT was expressed was measured with 0 mM KCl in the external buffer (closed squares). The values of the  $\text{K}^+$  equilibrium potentials are indicated.

obtained previously for Glt<sub>Ph</sub> ( $Q_{10}$  of 3.7) (31) and various other bacterial glutamate transporters ( $Q_{10}$ s of ~2.2) (M. Groeneveld, unpublished data), although the  $Q_{10}$  value for DctA<sub>BS</sub> is lower than those for the aforementioned proteins.

## DISCUSSION

Prokaryotic transporters of the DAACS family can be subdivided into three separate classes based on substrate specificity (33): glutamate/aspartate transporters, neutral amino acid transporters, and transporters for  $\text{C}_4$ -dicarboxylates of the Krebs cycle. Glutamate/aspartate transporters and the serine/threonine transporter SstT have been studied *in vitro* using membrane vesicles and purified proteins reconstituted into liposomes, but DctA-type dicarboxylate transporters have been studied in whole-cell assays only.

In this report, we describe the characterization of DctA<sub>BS</sub> in membrane vesicles from *L. lactis* in which DctA<sub>BS</sub> was overproduced. We observed DctA<sub>BS</sub>-specific succinate transport in these membranes, and a series of inhibition and counterflow assays showed that fumarate, malate, and oxaloacetate were also transported by DctA<sub>BS</sub>. The substrate specificity of DctA<sub>BS</sub> is narrower than that of other DctA homologues, which have been reported to transport other compounds such as orotate, glyoxylate, and  $\alpha$ -ketoglutarate (41, 42). None of these substrates were transported by DctA<sub>BS</sub>.

We made a homology model of the substrate-binding site of DctA<sub>Bs</sub> by using the crystal structure of Glt<sub>Ph</sub> as a template (data not shown). When the amino acids in Glt<sub>Ph</sub> involved in substrate binding (2) were compared with the corresponding amino acids in DctA<sub>Bs</sub>, only a few differences were found. The most obvious difference is the replacement of Asp394 from Glt<sub>Ph</sub> by Ser377 in DctA<sub>Bs</sub>. In Glt<sub>Ph</sub>, Asp394 interacts with the  $\alpha$ -amino group of the substrate aspartate, which is not present in the dicarboxylate substrates of DctA<sub>Bs</sub>. The binding pocket in Glt<sub>Ph</sub> for the two carboxylates of aspartate is strongly conserved in DctA<sub>Bs</sub>. The pH dependence of succinate transport by DctA<sub>Bs</sub> suggested that the doubly deprotonated (divalent anionic) form of succinate was recognized by the transporter, which would be consistent with the presence of a conserved binding site for the two carboxylate groups, because the divalent anionic form of aspartate is also transported by Glt<sub>Ph</sub> (2, 31).

Substrate transport by DctA<sub>Bs</sub> was coupled to proton transport (symport) and was not dependent on sodium ions. Succinate transport was stimulated by a negative membrane potential, indicating that transport was electrogenic. Therefore, at least three protons must be transported with the divalent anion succinate. This pattern is in contrast with succinate transport by the *Staphylococcus aureus* protein SdcS, a sodium-coupled C<sub>4</sub>-dicarboxylate transporter of the divalent anion:Na<sup>+</sup> symporter (DASS) family, which has been characterized using proteoliposomes containing purified protein. SdcS transports a doubly deprotonated substrate together with two sodium ions, resulting in electroneutral transport (13). On the other hand, transport by eukaryotic homologues of SdcS (members of the SIC13 subfamily) is electrogenic; three sodium ions are co-transported with a divalent substrate (25).

Glutamate/aspartate transporters of the DAACS family use either protons (in the case of GltP from *E. coli*) or sodium ions (in the case of Glt<sub>Ph</sub>) as coupling ions. Sodium ion binding by the aspartate transporter Glt<sub>Ph</sub>, for which a crystal structure has been determined, has been studied in detail. By using thallium ions to replace sodium in the crystals of Glt<sub>Ph</sub>, Boudker et al. found two distinct sodium-binding sites in the protein, in close proximity to the aspartate-binding site (2). We compared the sodium ion-binding sites in the crystal structure of Glt<sub>Ph</sub> with sites in the homology model of DctA<sub>Bs</sub> and found surprisingly few differences. In the first site, the sodium ion is coordinated by three backbone carbonyl oxygen atoms and a carboxylate from Asp405 in Glt<sub>Ph</sub>. This aspartate residue is conserved among human homologues (40), and another acidic residue (glutamate) is present in the binding site of the sodium-coupled serine/threonine transporter SstT from *E. coli*. Proton-coupled transporters such as DctA or bacterial glutamate transporters such as GltT from *B. stearothermophilus* (40) lack the aspartate residue in the first binding site and contain an asparagine residue instead. In the second predicted sodium-binding site, the sodium ion is coordinated by backbone carbonyls only (33, 40). The homology model of DctA<sub>Bs</sub> does not allow us to pinpoint the locations of the three proton-binding sites, but based on tertiary-structure conservation, it seems likely that the proton-binding sites in DctA are at positions similar to those of the predicted sodium-binding sites in Glt<sub>Ph</sub> (2). The third proton may bind in an additional ion-binding site, as predicted by Holley and Kavanaugh (15).

## ACKNOWLEDGMENTS

We thank Ruben Vis for his initial experiments with *E. coli* DctA and Guus Erkens for his kind gift of *L. lactis* cells harboring a ThiT expression vector.

This work was supported by a *vidi* grant from the Netherlands Organization for Scientific Research (NWO) to D.J.S.

## REFERENCES

- Asai, K., S. H. Baik, Y. Kasahara, S. Moriya, and N. Ogasawara. 2000. Regulation of the transport system for C<sub>4</sub>-dicarboxylic acids in *Bacillus subtilis*. *Microbiology* **146**(Pt. 2):263–271.
- Boudker, O., R. M. Ryan, D. Yernool, K. Shimamoto, and E. Gouaux. 2007. Coupling substrate and ion binding to extracellular gate of a sodium-dependent aspartate transporter. *Nature* **445**:387–393.
- Crisman, T., S. Qu, B. Kanner, and L. Forrest. 2009. Inward-facing conformation of glutamate transporters as revealed by their inverted-topology structural repeats. *Proc. Natl. Acad. Sci. U. S. A.* **106**:20752–20757.
- Danbolt, N. C. 2001. Glutamate uptake. *Prog. Neurobiol.* **65**:1–105.
- Davies, S. J., P. Golby, D. Omrani, S. A. Broad, V. L. Harrington, J. R. Guest, D. J. Kelly, and S. C. Andrews. 1999. Inactivation and regulation of the aerobic C<sub>4</sub>-dicarboxylate transport (*dctA*) gene of *Escherichia coli*. *J. Bacteriol.* **181**:5624–5635.
- Eudes, A., G. B. Erkens, D. J. Slotboom, D. A. Rodionov, V. Naponelli, and A. D. Hanson. 2008. Identification of genes encoding the folate- and thiamine-binding membrane proteins in Firmicutes. *J. Bacteriol.* **190**:7591–7594.
- Gaillard, I., D. J. Slotboom, J. Knol, J. S. Lokema, and W. N. Konings. 1996. Purification and reconstitution of the glutamate carrier GltT of the thermophilic bacterium *Bacillus stearothermophilus*. *Biochemistry* **35**:6150–6156.
- Geertsma, E. R., N. A. B. Nik Mahmood, G. K. Schuurman-Wolters, and B. Poolman. 2008. Membrane reconstitution of ABC transporters and assays of translocator function. *Nat. Protoc.* **3**:256–266.
- Geertsma, E. R., and B. Poolman. 2007. High-throughput cloning and expression in recalcitrant bacteria. *Nat. Methods* **4**:705–707.
- Gendreau, S., S. Voswinkel, D. Torres-Salazar, N. Lang, H. Heidtmann, S. Detro-Dassen, G. Schmalzing, P. Hidalgo, and C. Fahlke. 2004. A trimeric quaternary structure is conserved in bacterial and human glutamate transporters. *J. Biol. Chem.* **279**:39505–39512.
- Grewer, C., P. Balani, C. Weidenfeller, T. Bartusel, Z. Tao, and T. Rauen. 2005. Individual subunits of the glutamate transporter EAAC1 homotrimer function independently of each other. *Biochemistry* **44**:11913–11923.
- Groeneveld, M., and D.-J. Slotboom. 2007. Rigidity of the subunit interfaces of the trimeric glutamate transporter GltT during translocation. *J. Mol. Biol.* **372**:565–570.
- Hall, J. A., and A. M. Pajor. 2007. Functional reconstitution of SdcS, a Na<sup>+</sup>-coupled dicarboxylate carrier protein from *Staphylococcus aureus*. *J. Bacteriol.* **189**:880–885.
- Heuberger, E. H., E. Smits, and B. Poolman. 2001. Xyloside transport by XylP, a member of the galactoside-pentoside-hexuronide family. *J. Biol. Chem.* **276**:34465–34472.
- Holley, D. C., and M. P. Kavanaugh. 2009. Interactions of alkali cations with glutamate transporters. *Philos. Trans. R. Soc. Lond. B Biol. Sci.* **364**:155–161.
- Janausch, I. G., E. Zientz, Q. H. Tran, A. Kroger, and G. Uden. 2002. C<sub>4</sub>-dicarboxylate carriers and sensors in bacteria. *Biochim. Biophys. Acta* **1553**:39–56.
- Kim, Y.-M., W. Ogawa, E. Tamai, T. Kuroda, T. Mizushima, and T. Tsuchiya. 2002. Purification, reconstitution, and characterization of Na<sup>+</sup>/serine symporter, SstT, of *Escherichia coli*. *J. Biochem.* **132**:71–76.
- Koch, H. P., R. L. Brown, and H. P. Larsson. 2007. The glutamate-activated anion conductance in excitatory amino acid transporters is gated independently by the individual subunits. *J. Neurosci.* **27**:2943–2947.
- Koch, H. P., and H. P. Larsson. 2005. Small-scale molecular motions accomplish glutamate uptake in human glutamate transporters. *J. Neurosci.* **25**:1730–1736.
- Kuipers, O. P., M. M. Beerthuyzen, R. J. Siezen, and W. M. de Vos. 1993. Characterization of the nisin gene cluster *nisABTCIPR* of *Lactococcus lactis*. Requirement of expression of the *nisA* and *nisI* genes for development of immunity. *Eur. J. Biochem.* **216**:281–291.
- Kuipers, O. P., P. G. de Ruyter, M. Kleerebezem, and W. M. de Vos. 1998. Quorum sensing controlled gene expression in lactic acid bacteria. *J. Biotechnol.* **64**:15–21.
- Kunji, E. R. S., D.-J. Slotboom, and B. Poolman. 2003. *Lactococcus lactis* as host for overproduction of functional membrane proteins. *Biochim. Biophys. Acta* **1610**:97–108.
- Leary, G. P., E. F. Stone, D. C. Holley, and M. P. Kavanaugh. 2007. The glutamate and chloride permeation pathways are colocalized in individual neuronal glutamate transporter subunits. *J. Neurosci.* **27**:2938–2942.
- Levy, L. M., O. Warr, and D. Attwell. 1998. Stoichiometry of the glial glutamate transporter GLT-1 expressed inducibly in a Chinese hamster

- ovary cell line selected for low endogenous  $\text{Na}^+$ -dependent glutamate uptake. *J. Neurosci.* **18**:9620–9628.
25. **Markovich, D., and H. Murer.** 2004. The SLC13 gene family of sodium sulphate/carboxylate cotransporters. *Pflugers Arch.* **447**:594–602.
  26. **Poolman, B., E. J. Smid, and W. N. Konings.** 1987. Kinetic properties of a phosphate-bond-driven glutamate-glutamine transport system in *Streptococcus lactis* and *Streptococcus cremoris*. *J. Bacteriol.* **169**:2755–2761.
  27. **Prakash, S., G. Cooper, S. Singhi, and M. H. J. Saier.** 2003. The ion transporter superfamily. *Biochim. Biophys. Acta* **1618**:79–92.
  28. **Raunser, S., M. Appel, C. Ganea, U. Geldmacher-Kaufner, K. Fendler, and W. Kuhlbrandt.** 2006. Structure and function of prokaryotic glutamate transporters from *Escherichia coli* and *Pyrococcus horikoshii*. *Biochemistry* **45**:12796–12805.
  29. **Reyes, N., C. Ginter, and O. Boudker.** 2009. Transport mechanism of a bacterial homologue of glutamate transporters. *Nature* **462**:880–885.
  30. **Ronson, C. W., P. M. Astwood, and J. A. Downie.** 1984. Molecular cloning and genetic organization of  $\text{C}_4$ -dicarboxylate transport genes from *Rhizobium leguminosarum*. *J. Bacteriol.* **160**:903–909.
  31. **Ryan, R. M., E. L. R. Compton, and J. A. Mindell.** 2009. Functional characterization of a  $\text{Na}^+$ -dependent aspartate transporter from *Pyrococcus horikoshii*. *J. Biol. Chem.* **284**:17540–17548.
  32. **Saier, M. H. J., C. V. Tran, and R. D. Barabote.** 2006. TCDB: the Transporter Classification Database for membrane transport protein analyses and information. *Nucleic Acids Res.* **34**:D181–D186.
  33. **Slotboom, D., W. Konings, and J. Lolkema.** 1999. Structural features of the glutamate transporter family. *Microbiol. Mol. Biol. Rev.* **63**:293–307.
  34. **Tolner, B., T. Ubbink-Kok, B. Poolman, and W. N. Konings.** 1995. Cation-selectivity of the L-glutamate transporters of *Escherichia coli*, *Bacillus stearothermophilus* and *Bacillus caldopenax*: dependence on the environment in which the proteins are expressed. *Mol. Microbiol.* **18**:123–133.
  35. **Tolner, B., T. Ubbink-Kok, B. Poolman, and W. N. Konings.** 1995. Characterization of the proton/glutamate symport protein of *Bacillus subtilis* and its functional expression in *Escherichia coli*. *J. Bacteriol.* **177**:2863–2869.
  36. **Utsunomiya-Tate, N., H. Endou, and Y. Kanai.** 1996. Cloning and functional characterization of a system ASC-like  $\text{Na}^+$ -dependent neutral amino acid transporter. *J. Biol. Chem.* **271**:14883–14890.
  37. **van Slooten, J. C., T. V. Bhuvanavari, S. Bardin, and J. Stanley.** 1992. Two  $\text{C}_4$ -dicarboxylate transport systems in *Rhizobium* sp. NGR234: rhizobial dicarboxylate transport is essential for nitrogen fixation in tropical legume symbioses. *Mol. Plant Microbe Interact.* **5**:179–186.
  38. **Yarosh, O. K., T. C. Charles, and T. M. Finan.** 1989. Analysis of  $\text{C}_4$ -dicarboxylate transport genes in *Rhizobium meliloti*. *Mol. Microbiol.* **3**:813–823.
  39. **Yernool, D., O. Boudker, E. Folta-Stogniew, and E. Gouaux.** 2003. Trimeric subunit stoichiometry of the glutamate transporters from *Bacillus caldopenax* and *Bacillus stearothermophilus*. *Biochemistry* **42**:12981–12988.
  40. **Yernool, D., O. Boudker, Y. Jin, and E. Gouaux.** 2004. Structure of a glutamate transporter homologue from *Pyrococcus horikoshii*. *Nature* **431**:811–818.
  41. **Youn, J.-W., E. Jolkver, R. Kramer, K. Marin, and V. F. Wendisch.** 2009. Characterization of the dicarboxylate transporter DctA in *Corynebacterium glutamicum*. *J. Bacteriol.* **191**:5480–5488.
  42. **Yurgel, S., M. W. Mortimer, K. N. Rogers, and M. L. Kahn.** 2000. New substrates for the dicarboxylate transport system of *Sinorhizobium meliloti*. *J. Bacteriol.* **182**:4216–4221.
  43. **Yurgel, S. N., and M. L. Kahn.** 2004. Dicarboxylate transport by rhizobia. *FEMS Microbiol. Rev.* **28**:489–501.
  44. **Zerangue, N., and M. P. Kavanaugh.** 1996. ASCT-1 is a neutral amino acid exchanger with chloride channel activity. *J. Biol. Chem.* **271**:27991–27994.
  45. **Zerangue, N., and M. P. Kavanaugh.** 1996. Flux coupling in a neuronal glutamate transporter. *Nature* **383**:634–637.